

## **NRC Publications Archive** **Archives des publications du CNRC**

### **Rotational fine structure in the 0,0 and 0,1 bands of the O<sub>2</sub>( 1Δg- 3Σg<sup>-</sup>) system**

Gattinger, R. L.

For the publisher's version, please access the DOI link below./ Pour consulter la version de l'éditeur, utilisez le lien DOI ci-dessous.

#### **Publisher's version / Version de l'éditeur:**

<https://doi.org/10.4224/21277219>

*Report (National Research Council of Canada. Radio and Electrical Engineering Division : ERB), 1968-09*

#### **NRC Publications Archive Record / Notice des Archives des publications du CNRC :**

<https://nrc-publications.canada.ca/eng/view/object/?id=56f3c88f-1e91-4660-869f-cb9f41c03faf>

<https://publications-cnrc.canada.ca/fra/voir/objet/?id=56f3c88f-1e91-4660-869f-cb9f41c03faf>

Access and use of this website and the material on it are subject to the Terms and Conditions set forth at

<https://nrc-publications.canada.ca/eng/copyright>

READ THESE TERMS AND CONDITIONS CAREFULLY BEFORE USING THIS WEBSITE.

L'accès à ce site Web et l'utilisation de son contenu sont assujettis aux conditions présentées dans le site

<https://publications-cnrc.canada.ca/fra/droits>

LISEZ CES CONDITIONS ATTENTIVEMENT AVANT D'UTILISER CE SITE WEB.

**Questions?** Contact the NRC Publications Archive team at

PublicationsArchive-ArchivesPublications@nrc-cnrc.gc.ca. If you wish to email the authors directly, please see the first page of the publication for their contact information.

**Vous avez des questions?** Nous pouvons vous aider. Pour communiquer directement avec un auteur, consultez la première page de la revue dans laquelle son article a été publié afin de trouver ses coordonnées. Si vous n'arrivez pas à les repérer, communiquez avec nous à PublicationsArchive-ArchivesPublications@nrc-cnrc.gc.ca.



Ser C?  
QC1  
N21  
ERB  
no. 785

ERB-785

UNCLASSIFIED

NATIONAL RESEARCH COUNCIL OF CANADA  
RADIO AND ELECTRICAL ENGINEERING DIVISION

ANALYZED

ROTATIONAL FINE STRUCTURE IN THE 0,0 AND 0,1 BANDS  
OF THE  $O_2(^1\Delta_g - ^3\Sigma_g^-)$  SYSTEM

R. L. GATTINGER

ON LOAN  
from  
National Research Council  
Radio & E.E. Division  
Document Control Section

OTTAWA

SEPTEMBER 1968

NRC # 22169

*ANALYZED*

## ABSTRACT

The observations of the 0,0 ( $1.27\mu$ ) and 0,1 ( $1.58\mu$ ) bands of the  $O_2 (^1\Delta_g - ^3\Sigma_g^-)$  system arising from the airglow surrounding the earth have introduced the necessity for calculating the theoretical spectra of these two bands. All the necessary constants are available in the literature to a sufficient degree of accuracy, and the methods to be employed in calculating the spectra are well established. The wave-numbers in vacuum and wavelengths in air were calculated for all the important transitions in each band. The intensity of each rotational line was calculated for temperatures of  $200^{\circ}\text{K}$ ,  $250^{\circ}\text{K}$ , and  $300^{\circ}\text{K}$ . The transitions were arranged in order of wavelength, and then plotted after a triangular transmission function typical of a scanning grating spectrometer was applied.

## CONTENTS

	Page
Introduction . . . . .	1
Calculation of the energy levels in the $O_2(^3\Sigma_g^-)$ state . . . . .	2
Calculation of the energy levels in the $O_2(^1\Delta_g)$ state . . . . .	4
Calculation of the wavenumbers and wavelengths of the transitions in the 0,0 and 0,1 bands . . . . .	4
Calculation of the relative intensities of the transitions in each band . . . . .	11
Smearing and plotting of spectra . . . . .	11
Digital computer program . . . . .	12
Summary . . . . .	12
References . . . . .	12

## FIGURES

1. Sample of allowed (circled) energy levels and transitions in the  $O_2(^1\Delta_g - ^3\Sigma_g^-)$  system. The rotational transition scheme is identical for the 0,0 and 0,1 bands.
2. Theoretical spectrum of the 0,0 and 0,1 bands at 250°K after convolution with a triangular function with a full width of 2 Å at half-height.
3. Theoretical spectrum of the central portion of the 0,0 and 0,1 bands at 250°K after convolution with a triangular function with a full width of 2 Å at half-height.
4. Theoretical spectrum of the 0,0 and 0,1 bands at 300°K after convolution with a triangular function with a full width of 10 Å at half-height.
5. Theoretical spectrum of the 0,0 and 0,1 bands at 200°K after convolution with a triangular function with a full width of 50 Å at half-height.
6. Flow chart of the computer program written to solve the equations describing the band structure in the  $O_2(^1\Delta_g - ^3\Sigma_g^-)$  system.

## TABLES

- I Vibrational and rotational constants of the  $O_2(^3\Sigma_g^-)$  and  $O_2(^1\Delta_g)$  states.
- II Energy levels in the  $O_2(^3\Sigma_g^-)$  state in the two lowest vibrational levels.
- III Energy levels in the  $O_2(^1\Delta_g)$ ,  $\nu' = 0$  state.
- IV Changes in the quantum numbers  $J$  and  $K$  for the nine branches in each band of the  $O_2(^1\Delta_g - ^3\Sigma_g^-)$  system.
- V Wavenumbers (vacuum) and wavelengths (air) of the transitions in the 0,0 and 0,1 bands of the  $O_2(^1\Delta_g - ^3\Sigma_g^-)$  system.
- VI Relative populations in the rotational levels of the  $O_2(^1\Delta_g)$ ,  $\nu'=0$  state at various temperatures.
- VII Line strengths of the nine branches in each band as a function of the quantum number  $J'$  in the  $O_2(^1\Delta_g)$  state.
- VIII Relative intensities of rotational lines in the 0,0 and 0,1 bands of the  $O_2(^1\Delta_g - ^3\Sigma_g^-)$  system at various temperatures.

# ROTATIONAL FINE STRUCTURE IN THE 0,0 AND 0,1 BANDS

## OF THE $O_2(^1\Delta_g - ^3\Sigma_g^-)$ SYSTEM

— R.L. Gattinger —

### INTRODUCTION

The  $O_2(^1\Delta_g - ^3\Sigma_g^-)$  infrared atmospheric oxygen system, which originates in the airglow surrounding the earth, plays an important role in the photochemistry of the atmosphere. The observations of the 0,0 ( $1.27 \mu$ ) and 0,1 ( $1.58 \mu$ ) bands of this system have been reviewed recently by several authors (Hunten 1967; Evans 1967; Noxon 1968; Gattinger 1968). Both bands are emitted continually with the brightness of the 0,0 band being about 25 MR at local noon and about 100 kR during the late night hours. The 0,1 band is about 50 times weaker, but it is usually selected for ground-based observations because the 0,0 band is strongly absorbed by the  $O_2(^3\Sigma_g^-)$  molecules in the lower atmosphere. The  $O_2(^1\Delta_g)$  state has a lifetime of about 45 minutes, and this makes it possible to observe the emissions in the evening twilight airglow more readily than at dawn if there is an appreciable amount of scattered solar radiation in the field of view of the instrument.

The existence of the  $O_2(^1\Delta_g)$  state was suggested by Ellis and Kneser (1933) on the basis of the absorption spectrum of liquid oxygen, and also on the atmospheric absorption in the solar spectrum. The  $O_2(^1\Delta_g - ^3\Sigma_g^-)$  system was positively identified by Herzberg (1934) in a terrestrial solar spectrum which included the 0,0 band at  $1.27 \mu$ . A more accurate analysis of the  $O_2(^1\Delta_g - ^3\Sigma_g^-)$  system was presented by Herzberg and Herzberg (1947); they derived the required molecular constants of the  $O_2(^1\Delta_g)$  state to an accuracy which is sufficient for the present analysis.

An accurate set of molecular constants for the  $O_2(^3\Sigma_g^-)$  state was determined by Babcock and Herzberg (1948) from spectra of the  $O_2(^1\Sigma_g^+ - ^3\Sigma_g^-)$  system, commonly known as the atmospheric oxygen system.

The formulas required to calculate the wavenumbers in vacuum, wavelengths in air, and the relative intensities of the rotational lines in each band are readily available and will be discussed in the following sections. A digital computer program was written in the Fortran language to solve the necessary equations.

## CALCULATION OF THE ENERGY LEVELS IN THE $O_2(^3\Sigma_g^-)$ STATE

The contents of this section are based largely upon the results obtained by Babcock and Herzberg (1948). The fine structure of the  $O_2(^3\Sigma_g^-)$  state is shown in Fig. 1. The rotational levels with even values of  $K''$  are absent, and those with odd values of  $K''$  are split into three levels,  $F_1''(K)$ ,  $F_2''(K)$ , and  $F_3''(K)$ , corresponding to the cases where  $J'' = K'' + 1$ ,  $J'' = K''$ , and  $J'' = K'' - 1$ , respectively. The formulas for these levels in a  $^3\Sigma$  state are as follows (Babcock and Herzberg 1948):

$$F_2''(K) = B_\nu K''(K'' + 1) - D_\nu K''^2(K'' + 1)^2 \quad (1)$$

$$\begin{aligned} F_1''(K) &= F_2''(K) + (2K'' + 3)B_\nu - \lambda_\nu \\ &\quad - [(2K'' + 3)^2 B_\nu^2 + \lambda_\nu^2 - 2\lambda_\nu B_\nu]^{1/2} + \gamma(K'' + 1) \end{aligned} \quad (2)$$

$$\begin{aligned} F_3''(K) &= F_2''(K) - (2K'' - 1)B_\nu - \lambda_\nu \\ &\quad + [(2K'' - 1)^2 B_\nu^2 + \lambda_\nu^2 - 2\lambda_\nu B_\nu]^{1/2} - \gamma K''. \end{aligned} \quad (3)$$

The constants required to evaluate these expressions are given in Table I. The rotational energy levels are referred to the non-existent  $F_2''(0)$  state in the vibrational energy level concerned.

The energy separation,  $\Delta G_{1/2}$ , between the two lowest vibrational levels is also given in Table I. It is of interest to note that Harrison (1957) used a value of  $1556.2153 \text{ cm}^{-1}$  which was derived using the formula (Herzberg (1950); formula III, 81)

$$\Delta G_{1/2} = \omega_e - 2\omega_e x_e \quad (4)$$

However, the formula (Herzberg (1950); formula III, 81a)

$$\Delta G_{1/2} = \omega_e - 2\omega_e x_e + 3.25 \omega_e y_e + 5\omega_e z_e \quad (5)$$

must be used to obtain the value of  $\Delta G_{1/2}$  given in Table I.

The energy of the non-existent  $F_2''(0)$  state in the lowest vibrational level of the  $O_2(^3\Sigma_g^-)$  state was set equal to zero, and all other levels were referred to this state; the

Table I

Vibrational and rotational constants of the  $O_2(^3\Sigma_g^-)$  and  $O_2(^1\Delta_g)$  states

Constant	$^3\Sigma_g^-$ ( $\text{cm}^{-1}$ )	$^1\Delta_g$ ( $\text{cm}^{-1}$ )
$\Delta G_{1/2}$	1556.3856	
$A_0 = \nu_{00}$		7882.39
$\omega_e$	1580.3613	
$\omega_e x_e$	12.0730	
$\omega_e y_e$	0.0546	
$\omega_e z_e$	-0.00143	
$B_0$	1.437770	1.41783
$B_1$	1.421979	
$D_0$	$4.913 \times 10^{-6}$	$4.86 \times 10^{-6}$
$D_1$	$4.825 \times 10^{-6}$	
$\lambda_0$	1.984	
$\lambda_1$	1.993	
$\gamma$	-0.00837	

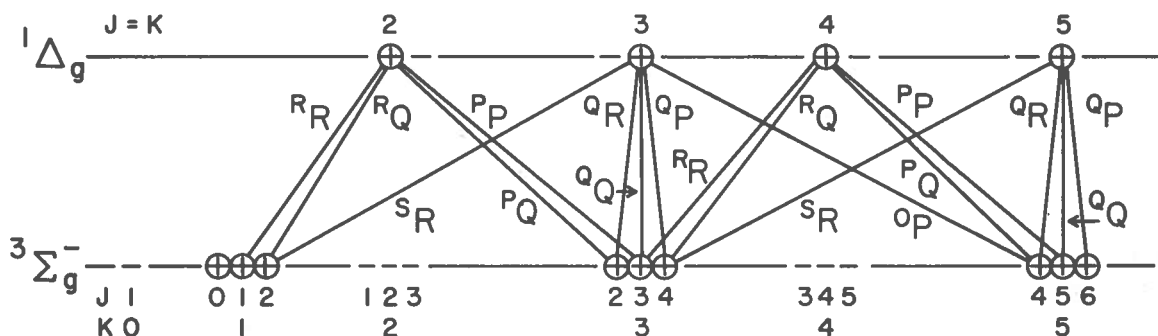


Fig. 1 Sample of allowed (circled) energy levels and transitions in the  $O_2(^1\Delta_g - ^3\Sigma_g^-)$  system. The rotational transition scheme is identical for the 0,0 and 0,1 bands.

quantity  $\Delta G_{\frac{1}{2}}$  was added to each of the rotational energy levels calculated for the state  $v'' = 1$  to make this condition true for both vibrational levels. The energy levels are listed in Table II.

### CALCULATION OF THE ENERGY LEVELS IN THE $O_2(^1\Delta_g)$ STATE

The results of Herzberg and Herzberg (1947) were used to calculate the energy levels in the  $O_2(^1\Delta_g)$  state. The rotational fine structure of this state is shown in Fig. 1. In a singlet state,  $J' = K'$ , since the spin,  $S = 0$ ; also, in a  $\Delta$  state the levels,  $J' = 0$  and  $J' = 1$ , are absent. Only the positive rotational levels occur, and in these calculations the  $\lambda$  doubling has been ignored. The formula for the calculation of the rotational energy levels is (Herzberg (1950); formula III, 104)

$$F'(J) = B_v J' (J' + 1) - D_v J'^2 (J' + 1)^2 \quad (6)$$

which refers the levels to the non-existent  $F'(0)$  level. These  $O_2(^1\Delta_g)$  levels were referred to the non-existent  $O_2(^3\Sigma_g^-)$ ,  $v'' = 0$ ,  $F_2''(0)$  level by adding the term,  $v_{00}$ , for the  $O_2(^1\Delta_g - ^3\Sigma_g^-)$  system to each of the rotational levels in the  $O_2(^1\Delta_g)$  state. The constants required for these calculations are given in Table I, and the calculated energy levels are given in Table III.

### CALCULATION OF THE WAVENUMBERS AND WAVELENGTHS OF THE TRANSITIONS IN THE 0,0 AND 0,1 BANDS

Examples of the types of transitions which occur in the  $O_2(^1\Delta_g - ^3\Sigma_g^-)$  system (Herzberg and Herzberg (1947)) are shown in Fig. 1. Each band contains nine branches, and the changes in the quantum numbers,  $J$  and  $K$ , corresponding to each branch are given in Table IV. The wavenumbers in vacuum of the transitions in each branch of the two bands, calculated by determining the difference in energy between the upper and lower levels involved, are given in Table V.

The wavelengths in air, also given in Table V, were calculated with the formula for the refractive index of air given by Coleman, Bozman, and Meggers (1960); page 4,

$$n = 1 + 6432.8 \times 10^{-8} + \frac{2949810}{146 \times 10^8 - \sigma^2} + \frac{-25540}{41 \times 10^8 - \sigma^2} \quad (7)$$

where  $\sigma$  is the vacuum wavenumber.

The good agreement between the results given in Table V and those given by Herzberg and Herzberg (1947) and Mohler (1955) indicates that the methods employed are correct.

Table II

Energy levels in the  $O_2(^3\Sigma_g^-)$  state in the two lowest vibrational levels

K	SIGMA	STATE	V = 0	K	SIGMA	STATE	V = 1
	F1(K)	F2(K)	F3(K)		F1(K)	F2(K)	F3(K)
1	0.9989	2.8755	0.0083	1	1557.3394	1559.2292	1556.3931
3	15.3036	17.2525	15.1695	3	1571.4878	1573.4485	1571.3596
5	41.1418	43.1287	41.1179	5	1597.0425	1599.0403	1597.0222
7	78.4849	80.4997	78.5269	7	1633.9756	1636.0010	1634.0200
9	127.3211	129.3595	127.4146	9	1682.2756	1684.3245	1682.3711
11	187.6402	189.7000	187.7787	11	1741.9324	1744.0024	1742.0728
13	259.4307	261.5110	259.6108	13	1812.9358	1815.0256	1813.1169
15	342.6816	344.7815	342.9016	15	1895.2732	1897.3823	1895.4939
17	437.3784	439.4971	437.6362	17	1988.9307	1991.0588	1989.1895
19	543.5063	545.6431	543.8010	19	2093.8943	2096.0405	2094.1899
21	661.0457	663.2007	661.3767	21	2210.1453	2212.3096	2210.4771
23	789.9790	792.1516	790.3459	23	2337.6653	2339.8474	2338.0330
25	930.2839	932.4744	930.6865	25	2476.4331	2478.6331	2476.8367
27	1081.9377	1084.1455	1082.3752	27	2626.4260	2628.6433	2626.8645
29	1244.9153	1247.1406	1245.3882	29	2787.6199	2789.8547	2788.0935
31	1419.1899	1421.4329	1419.6975	31	2959.9880	2962.2402	2960.4963
33	1604.7322	1606.9922	1605.2744	33	3143.5020	3145.7712	3144.0447
35	1801.5125	1803.7898	1802.0891	35	3338.1318	3340.4185	3338.7090
37	2009.4973	2011.7917	2010.1084	37	3543.8457	3546.1494	3544.4573
39	2228.6523	2230.9641	2229.2981	39	3760.6089	3762.9299	3761.2551
41	2458.9421	2461.2710	2459.6221	41	3988.3811	3990.7253	3989.0676
43	2700.3276	2702.6733	2701.0417	43	4227.1328	4229.4961	4227.8477
45	2952.7683	2955.1311	2953.5161	45	4476.8242	4479.2031	4477.5703
47	3216.2239	3218.6038	3217.0061	47	4737.4180	4739.8125	4738.1953
49	3490.6482	3493.0452	3491.4644	49	5008.8516	5011.2695	5009.6680
51	3775.9983	3778.4119	3776.8481	51	5291.1016	5293.5352	5291.9570
53	4072.2195	4074.6521	4073.1052	53	5584.1172	5586.5664	5585.0039

Table III

Energy levels in the  $O_2(^1\Delta_g)$ ,  $v' = 0$  state

DELTA	STATE	V = 0		
K		F(K)		
2		7890.89	28	9030.46
3		7899.40	29	9112.22
4		7910.74	30	9196.76
5		7924.91	31	9284.09
6		7941.93	32	9374.19
7		7961.77	33	9467.07
8		7984.44	34	9562.72
9		8009.95	35	9661.13
10		8038.29	36	9762.31
11		8069.45	37	9866.25
12		8103.45	38	9972.93
13		8140.27	39	10082.37
14		8179.91	40	10194.55
15		8222.38	41	10309.48
16		8267.68	42	10427.13
17		8315.79	43	10547.52
18		8366.71	44	10670.63
19		8420.46	45	10796.47
20		8477.02	46	10925.02
21		8536.38	47	11056.27
22		8598.56	48	11190.23
23		8663.55	49	11326.89
24		8731.33	50	11466.25
25		8801.92	51	11608.29
26		8875.30	52	11753.01
27		8951.48	53	11900.40
			54	12050.47

Table IV

Changes in the quantum numbers  $J$  and  $K$  for the nine branches in each band of the  $O_2(^1\Delta_g - ^3\Sigma_g^-)$  system

<del><math>K' - K''</math></del> $J' - J''$	-2	-1	0	+1	+2
-1	$^0P$	$^P_P$	$^Q_P$		
0		$^P_Q$	$^Q_Q$	$^R_Q$	
+1			$^Q_R$	$^R_R$	$^S_R$

Table Va

Wavenumbers (vacuum) and wavelengths (air) of the transitions  
in the 0,0 band of the  $O_2(^1\Delta_g - ^3\Sigma_g^-)$  system

0-0 BAND				
J	RR	RQ	PP	PQ
2	7888.01	7889.89	7873.64	7875.72
2	12674.02	12671.00	12697.16	12693.80
4	7893.48	7895.43	7867.61	7869.62
4	12665.23	12662.11	12706.88	12703.64
6	7898.80	7900.78	7861.43	7863.40
6	12656.71	12653.53	12716.88	12713.69
8	7903.94	7905.95	7855.08	7857.02
8	12648.48	12645.25	12727.15	12724.00
10	7908.93	7910.96	7848.59	7850.51
10	12640.50	12637.25	12737.68	12734.57
12	7913.75	7915.81	7841.94	7843.84
12	12632.80	12629.51	12748.48	12745.39
14	7918.40	7920.48	7835.13	7837.01
14	12625.37	12622.06	12759.56	12756.50
16	7922.89	7924.99	7828.18	7830.04
16	12618.22	12614.87	12770.89	12767.86
18	7927.21	7929.34	7821.07	7822.91
18	12611.34	12607.96	12782.50	12779.49
20	7931.37	7933.51	7813.81	7815.64
20	12604.73	12601.34	12794.37	12791.38
22	7935.36	7937.52	7806.41	7808.21
22	12598.39	12594.97	12806.50	12803.54
24	7939.18	7941.35	7798.86	7800.64
24	12592.34	12588.89	12818.91	12815.97
26	7942.83	7945.02	7791.16	7792.93
26	12586.55	12583.08	12831.57	12828.66
28	7946.31	7948.52	7783.32	7785.07
28	12581.04	12577.54	12844.50	12841.61
30	7949.62	7951.84	7775.33	7777.06
30	12575.80	12572.28	12857.70	12854.83
32	7952.76	7955.00	7767.20	7768.91
32	12570.84	12567.29	12871.15	12868.31
34	7955.73	7957.98	7758.93	7760.63
34	12566.14	12562.58	12884.88	12882.05
36	7958.52	7960.80	7750.52	7752.20
36	12561.73	12558.14	12898.85	12896.05
38	7961.14	7963.43	7741.97	7743.63
38	12557.60	12553.98	12913.10	12910.32
40	7963.59	7965.90	7733.28	7734.93
40	12553.73	12550.09	12927.61	12924.85
42	7965.86	7968.19	7724.46	7726.09
42	12550.16	12546.49	12942.37	12939.64
44	7967.96	7970.30	7715.50	7717.11
44	12546.86	12543.16	12957.40	12954.69
46	7969.88	7972.25	7706.41	7708.01
46	12543.82	12540.11	12972.68	12969.99
48	7971.63	7974.01	7697.19	7698.77
48	12541.07	12537.34	12988.23	12985.55
50	7973.20	7975.60	7687.83	7689.39
50	12538.61	12534.84	13004.03	13001.39
52	7974.59	7977.01	7678.36	7679.90
52	12536.41	12532.62	13020.08	13017.46

Table Va continued

J	QR	QQ	QP	OP	SR
3	7884.23	7882.14	7884.09	7858.28	7898.40
3	12680.10	12683.45	12680.32	12721.97	12657.35
5	7883.79	7881.79	7883.77	7846.39	7909.61
5	12680.80	12684.03	12680.84	12741.25	12639.41
7	7883.24	7881.27	7883.28	7834.35	7920.62
7	12681.69	12684.86	12681.62	12760.82	12621.83
9	7882.53	7880.59	7882.62	7822.17	7931.46
9	12682.83	12685.95	12682.68	12780.70	12604.59
11	7881.67	7879.75	7881.81	7809.84	7942.13
11	12684.21	12687.30	12683.98	12800.88	12587.66
13	7880.66	7878.76	7880.84	7797.37	7952.63
13	12685.85	12688.90	12685.56	12821.36	12571.04
15	7879.48	7877.60	7879.70	7784.75	7962.95
15	12687.74	12690.77	12687.39	12842.14	12554.75
17	7878.15	7876.29	7878.41	7771.98	7973.10
17	12689.89	12692.89	12689.47	12863.23	12538.76
19	7876.65	7874.81	7876.95	7759.08	7983.08
19	12692.30	12695.26	12691.82	12884.62	12523.09
21	7875.00	7873.18	7875.34	7746.04	7992.87
21	12694.95	12697.89	12694.42	12906.32	12507.74
23	7873.20	7871.39	7873.57	7732.86	8002.50
23	12697.86	12700.77	12697.27	12928.31	12492.70
25	7871.23	7869.45	7871.64	7719.54	8011.94
25	12701.03	12703.92	12700.38	12950.61	12477.97
27	7869.11	7867.34	7869.54	7706.09	8021.20
27	12704.47	12707.32	12703.76	12973.21	12463.57
29	7866.83	7865.08	7867.30	7692.52	8030.28
29	12708.14	12710.97	12707.38	12996.11	12449.48
31	7864.39	7862.66	7864.90	7678.81	8039.17
31	12712.09	12714.89	12711.26	13019.30	12435.71
33	7861.79	7860.08	7862.34	7664.98	8047.88
33	12716.29	12719.06	12715.41	13042.80	12422.25
35	7859.04	7857.34	7859.62	7651.02	8056.40
35	12720.73	12723.49	12719.80	13066.59	12409.12
37	7856.14	7854.45	7856.75	7636.95	8064.73
37	12725.44	12728.17	12724.45	13090.68	12396.30
39	7853.07	7851.41	7853.72	7622.75	8072.87
39	12730.41	12733.11	12729.36	13115.06	12383.80
41	7849.85	7848.20	7850.53	7608.43	8080.82
41	12735.63	12738.30	12734.53	13139.73	12371.61
43	7846.48	7844.84	7847.19	7594.00	8088.57
43	12741.11	12743.76	12739.95	13164.71	12359.76
45	7842.95	7841.34	7843.70	7579.46	8096.14
45	12746.84	12749.46	12745.62	13189.96	12348.20
47	7839.27	7837.67	7840.05	7564.81	8103.50
47	12752.83	12755.43	12751.55	13215.51	12336.98
49	7835.43	7833.85	7836.25	7550.04	8110.67
49	12759.07	12761.65	12757.74	13241.36	12326.09
51	7831.44	7829.87	7832.29	7535.18	8117.64
51	12765.57	12768.12	12764.19	13267.46	12315.50

Table Vb

Wavenumbers (vacuum) and wavelengths (air) of the transitions  
in the 0,1 band of the  $O_2(^1\Delta_g - ^3\Sigma_g^-)$  system

0-1 BAND				
J	RR	RQ	PP	PQ
2	6331.66	6333.55	6317.44	6319.53
2	15789.35	15784.64	15824.89	15819.66
4	6337.29	6339.25	6311.70	6313.71
4	15775.33	15770.45	15839.30	15834.23
6	6342.88	6344.88	6305.92	6307.90
6	15761.41	15756.45	15853.80	15848.82
8	6348.44	6350.46	6300.11	6302.07
8	15747.62	15742.60	15868.41	15863.49
10	6353.96	6356.01	6294.29	6296.21
10	15733.93	15728.86	15883.11	15878.24
12	6359.45	6361.52	6288.42	6290.33
12	15720.36	15715.25	15897.91	15893.09
14	6364.89	6366.98	6282.53	6284.42
14	15706.93	15701.77	15912.82	15908.05
16	6370.29	6372.40	6276.61	6278.48
16	15693.59	15688.40	15927.83	15923.08
18	6375.65	6377.78	6270.67	6272.52
18	15680.40	15675.17	15942.92	15938.21
20	6380.97	6383.12	6264.70	6266.54
20	15667.33	15662.06	15958.11	15953.44
22	6386.25	6388.41	6258.71	6260.53
22	15654.38	15649.08	15973.37	15968.75
24	6391.48	6393.66	6252.70	6254.49
24	15641.56	15636.23	15988.75	15984.16
26	6396.67	6398.87	6246.66	6248.44
26	15628.89	15623.51	16004.20	15999.65
28	6401.81	6404.03	6240.60	6242.36
28	15616.33	15610.93	16019.74	16015.22
30	6406.91	6409.14	6234.52	6236.26
30	15603.91	15598.47	16035.37	16030.89
32	6411.95	6414.20	6228.42	6230.14
32	15591.64	15586.16	16051.08	16046.52
34	6416.95	6419.21	6222.30	6224.01
34	15579.50	15573.99	16066.87	16062.45
36	6421.89	6424.18	6216.16	6217.85
36	15567.50	15561.96	16082.73	16078.35
38	6426.78	6429.09	6210.00	6211.68
38	15555.66	15550.08	16098.68	16094.34
40	6431.62	6433.95	6203.83	6205.48
40	15543.95	15538.34	16114.70	16110.39
42	6436.41	6438.75	6197.64	6199.29
42	15532.39	15526.74	16130.80	16126.50
44	6441.14	6443.50	6191.43	6193.06
44	15520.99	15515.30	16146.96	16142.71
46	6445.81	6448.19	6185.20	6186.82
46	15509.73	15504.01	16163.22	16159.00
48	6450.42	6452.82	6178.96	6180.57
48	15498.64	15492.89	16179.54	16175.35
50	6454.98	6457.39	6172.71	6174.29
50	15487.71	15481.91	16195.93	16191.79
52	6459.47	6461.91	6166.44	6168.00
52	15476.93	15471.10	16212.40	16208.29

Table Vb continued

J	QR	QQ	QP	OP	SR
3	6328.04	6325.95	6327.91	6302.37	6342.06
3	15798.40	15803.61	15798.71	15862.72	15763.46
5	6327.89	6325.87	6327.87	6290.89	6353.43
5	15798.76	15803.80	15798.80	15891.68	15735.26
7	6327.75	6325.77	6327.79	6279.40	6364.73
7	15799.12	15804.07	15799.00	15920.76	15707.32
9	6327.58	6325.62	6327.67	6267.87	6375.97
9	15799.54	15804.43	15799.30	15950.03	15679.62
11	6327.38	6325.45	6327.52	6256.34	6387.18
11	15800.04	15804.86	15799.68	15979.45	15652.11
13	6327.15	6325.24	6327.33	6244.77	6398.34
13	15800.60	15805.37	15800.15	16009.04	15624.81
15	6326.89	6325.00	6327.11	6233.19	6409.45
15	15801.26	15805.98	15800.71	16038.79	15597.73
17	6326.59	6324.72	6326.85	6221.59	6420.51
17	15802.00	15806.67	15801.35	16068.68	15570.85
19	6326.27	6324.41	6326.56	6209.98	6431.52
19	15802.82	15807.44	15802.07	16098.74	15544.19
21	6325.90	6324.07	6326.23	6198.35	6442.49
21	15803.72	15808.30	15802.89	16128.95	15517.73
23	6325.51	6323.70	6325.88	6186.71	6453.40
23	15804.70	15809.23	15803.78	16159.29	15491.50
25	6325.08	6323.29	6325.49	6175.05	6464.25
25	15805.77	15810.26	15804.76	16189.79	15465.48
27	6324.62	6322.84	6325.05	6163.39	6475.05
27	15806.93	15811.38	15805.84	16220.43	15439.70
29	6324.12	6322.36	6324.60	6151.72	6485.79
29	15808.16	15812.57	15806.98	16251.20	15414.13
31	6323.59	6321.85	6324.10	6140.04	6496.47
31	15809.50	15813.86	15808.22	16282.10	15388.79
33	6323.02	6321.30	6323.57	6128.36	6507.08
33	15810.92	15815.24	15809.56	16313.14	15363.69
35	6322.42	6320.71	6323.00	6116.67	6517.63
35	15812.42	15816.70	15810.98	16344.32	15338.83
37	6321.79	6320.09	6322.40	6104.99	6528.11
37	15814.02	15818.25	15812.48	16375.59	15314.20
39	6321.11	6319.44	6321.76	6093.30	6538.52
39	15815.70	15819.89	15814.07	16407.00	15289.82
41	6320.41	6318.75	6321.09	6081.63	6548.87
41	15817.46	15821.61	15815.75	16438.49	15265.66
43	6319.67	6318.02	6320.39	6069.95	6559.14
43	15819.30	15823.43	15817.52	16470.12	15241.76
45	6318.90	6317.27	6319.64	6058.27	6569.34
45	15821.24	15825.33	15819.37	16501.86	15218.10
47	6318.08	6316.46	6318.86	6046.61	6579.45
47	15823.29	15827.34	15821.35	16533.71	15194.71
49	6317.23	6315.62	6318.04	6034.94	6589.48
49	15825.43	15829.44	15823.38	16565.67	15171.59
51	6316.33	6314.75	6317.19	6023.29	6599.44
51	15827.67	15831.62	15825.52	16597.72	15148.69

## CALCULATION OF THE RELATIVE INTENSITIES OF THE TRANSITIONS IN EACH BAND

The intensity of an emission line in units of energy is given by Herzberg (1950); formula I, 46,

$$I_{J'J''} = N_{J'} \ h c v_{J'J''} A_{J'J''}, \quad (8)$$

where  $N_{J'}$  is the population in the upper state and  $A_{J'J''}$  is the Einstein transition probability of spontaneous emission.

The relative populations of the rotational levels in the  $O_2(^1\Delta_g)$  state were calculated using the simplified relationship (Herzberg (1950); formula III, 161)

$$N_{J'} = (2J' + 1) \exp [ - (F'(J) - v_{00}) hc/kT ] \quad (9)$$

where the energy levels are referred to the non-existent  $F'(0)$  state. The relative populations obtained for various temperatures are given in Table VI.

The expression for  $A_{J'J''}$  (Herzberg (1950); formula I, 54; also page 127) was approximated by

$$A_{J'J''} \propto \frac{v_{J'J''}^3 S_J}{2J' + 1} \quad (10)$$

The line strength values,  $S_J$ , are given in Table VII (Van Vleck (1934)).

The relative intensities of the rotational lines given in Table VIII in photon units and at various temperatures were calculated using the expression

$$I_{J'J''} = C N_{J'} v_{J'J''}^3 \frac{S_J}{2J' + 1}, \quad (11)$$

where  $C$  was chosen so that the results would be in a convenient range.

## SMEARING AND PLOTTING OF SPECTRA

All the transitions in each band were arranged in wavelength order within the computer program to facilitate the convolution with an instrumental smearing function, and also to plot the resultant spectrum. To simplify the Fortran coding required to do this, the wavelengths were rounded to the nearest  $\frac{1}{4}$  Å; this introduced a maximum wavelength error of  $1/8$  Å. A triangular smearing function typical of a scanning grating spectrometer with a given spectral slit width was applied to each spectrum by the Fortran program, and the spectra were then automatically plotted on a digital plotter.

The spectra in Figs. 2 and 3 were calculated for a temperature of 250°K, and for a triangular smearing function of 2 Å full width at half-height. Figure 3 shows the central portion of each band on an expanded scale.

The spectra in Fig. 4 correspond to a temperature of 300°K with a 10-Å triangular smearing function. The 10 Å on either end of each band were not plotted because only those transitions occurring within a 500-Å interval were considered when smearing the spectrum. The spectral shape is very similar to that derived by Gush and Buijs (1964).

A temperature of 200°K and a 50-Å smearing function were used to derive the spectra in Fig. 5. Here again the 50 Å on either end of each band were not plotted since this would require information on transitions outside the 500-Å range assumed for the smearing function.

#### DIGITAL COMPUTER PROGRAM

A simplified flow chart of the program is given in Fig. 6. The time required to compile and execute the program for one temperature and one band pair is approximately 3 minutes. The plotting of the spectra on an off-line digital plotter requires from 10 to 20 minutes per band pair depending upon the number of points to be plotted.

#### SUMMARY

The theoretical spectra of the 0,0 and 0,1 bands of the  $O_2(^1\Delta_g - ^3\Sigma_g^-)$  system have been calculated to aid in the analysis of the observations of these emissions. A positive identification of the observed emissions is made possible by a direct comparison between the observed and theoretical spectra. Also, if the instrument used to make the observations does not exhibit a linear response at all wavelengths, the observed brightness may be corrected in accordance with the theoretical spectral information so that the total band brightness and possibly the true band shape may be derived. The theoretical results in this report have been presented in various forms to facilitate the comparison between the experimental and theoretical spectra.

#### REFERENCES

1. Babcock, H.D. and Herzberg, L. *Astrophys. J.* 108, 167. 1948
2. Coleman, C.D., Bozman, W.R., and Meggers, W.F. *Table of Wavenumbers (United States Government Printing Office)*. 1960
3. Ellis, J.W. and Kneser, H.O. *Z. Phys.* 86, 583. 1933
4. Evans, W.F.J. *Ph.D. Thesis, University of Saskatchewan*. 1967
5. Gattinger, R.L. *Can. J. Phys.* 46, 1613. 1968
6. Gush, H.P. and Buijs, H.L. *Can. J. Phys.* 42, 1037. 1964
7. Harrison, A.W. *Ph.D. Thesis, University of Saskatchewan*. 1957
8. Herzberg, G. *Nature* 133, 759. 1934
9. Herzberg, G. *Spectra of Diatomic Molecules (D. Van Nostrand Co. Inc.)*. 1950

10. Herzberg, G. and Herzberg, L. *Astrophys. J.* 105, 356. 1947
11. Hunten, D.M. *Space Sci. Rev.* 6, 493. 1967
12. Mohler, O.C. *A Table of Solar Spectrum Wavelengths, 11984Å to 25578Å* (University of Michigan Press, Ann Arbor, Michigan). 1955
13. Noxon, J.F. *Space Sci. Rev.* 8, 92. 1968
14. Van Vleck, J.H. *Astrophys. J.* 80, 161. 1934

Table VI

Relative populations in the rotational levels of the  $O_2(^1\Delta_g)$ ,  $\nu' = 0$  state at various temperatures

J	TEMP = 200.0°K	POPULATION	J	TEMP = 250.0°K	POPULATION
2		4.70327	2		4.76118
3		6.19365	3		6.34712
4		7.33941	4		7.64499
5		8.10066	5		8.61182
6		8.47070	6		9.22835
7		8.47359	7		9.49888
8		8.15810	8		9.44846
9		7.58922	9		9.11819
10		6.84097	10		8.56127
11		5.98767	11		7.83704
12		5.09627	12		7.00471
13		4.22313	13		6.12041
14		3.41039	14		5.23266
15		2.68583	15		4.38061
16		2.06403	16		3.59316
17		1.54867	17		2.88922
18		1.13492	18		2.27831
19		0.81268	19		1.76257
20		0.56875	20		1.33813
21		0.38915	21		0.99722
22		0.26037	22		0.72965
23		0.17039	23		0.52429
24		0.10908	24		0.37003
25		0.06832	25		0.25655
26		0.04188	26		0.17477
27		0.02512	27		0.11699
28		0.01475	28		0.07696
29		0.00848	29		0.04976
30		0.00477	30		0.03162
31		0.00263	31		0.01976
32		0.00142	32		0.01214
33		0.00075	33		0.00733
34		0.00039	34		0.00435
35		0.00020	35		0.00254
36		0.00010	36		0.00146
37		0.00005	37		0.00082
38		0.00002	38		0.00046
39		0.00001	39		0.00025
40		0.00000	40		0.00013
41		0.00000	41		0.00007
42		0.00000	42		0.00004
43		0.00000	43		0.00002
44		0.00000	44		0.00001
45		0.00000	45		0.00000
46		0.00000	46		0.00000
47		0.00000	47		0.00000
48		0.00000	48		0.00000
49		0.00000	49		0.00000
50		0.00000	50		0.00000
51		0.00000	51		0.00000
52		0.00000	52		0.00000
53		0.00000	53		0.00000
54		0.00000	54		0.00000
55		0.00000	55		0.00000

Table VI (continued) TEMP = 300.0°K

J	POPULATION		
2	4.80017	29	0.16188
3	6.45155	30	0.11158
4	7.85576	31	0.07580
5	8.97038	32	0.05077
6	9.77074	33	0.03352
7	10.25043	34	0.02182
8	10.42019	35	0.01400
9	10.30503	36	0.00886
10	9.94226	37	0.00553
11	9.37737	38	0.00340
12	8.65928	39	0.00207
13	7.83811	40	0.00124
14	6.96096	41	0.00073
15	6.06978	42	0.00043
16	5.19975	43	0.00024
17	4.37853	44	0.00014
18	3.62559	45	0.00008
19	2.95325	46	0.00004
20	2.36707	47	0.00002
21	1.86740	48	0.00001
22	1.45033	49	0.00000
23	1.10916	50	0.00000
24	0.83541	51	0.00000
25	0.61978	52	0.00000
26	0.45299	53	0.00000
27	0.32621	54	0.00000
28	0.23148	55	0.00000

Table VII

Line strengths of the nine branches in each band as a function of  
the quantum numbers in the  $O_2(^1\Delta_g)$  state

<del><math>K' - K''</math></del> $J' - J''$	-2	-1	0	+1	+2
-1	$\frac{(J'-1) J'}{2J'+3}$	$\frac{(J'-1) J'}{J'+1}$	$\frac{(J'-1) J' (J'+2)}{(J'+1) (2J'+3)}$		
0		$\frac{(J'+2) (J'-1)}{J'+1}$	$\frac{(J'+2) (J'-1) (2J'+1)}{J' (J'+1)}$	$\frac{(J'+2) (J'-1)}{J'}$	
+1			$\frac{(J'-1) (J'+1) (J'+2)}{J' (2J'-1)}$	$\frac{(J'+1) (J'+2)}{J'}$	$\frac{(J'+1) (J'+2)}{2J'-1}$

Table VIII

Relative intensities of rotational lines in the 0,0 and 0,1 bands of the  $O_2(^1\Delta_g - ^3\Sigma_g^-)$  system at various temperatures

0,0 BAND TEMP 200°K

J	RR	RQ	PP	PQ	
2	8.0759	2.6939	0.8924	1.7863	
4	8.7698	5.2658	2.7788	4.1714	
6	8.7378	6.2460	3.9556	5.2781	
8	7.7719	6.0495	4.2193	5.2781	
10	6.2020	5.0783	3.7569	4.5116	
12	4.4674	3.7831	2.9102	3.3977	
14	2.9181	2.5310	2.0009	2.2884	
16	1.7344	1.5316	1.2350	1.3903	
18	0.9405	0.8421	0.6890	0.7661	
20	0.4661	0.4221	0.3491	0.3843	
22	0.2115	0.1933	0.1612	0.1760	
24	0.0880	0.0810	0.0680	0.0737	
26	0.0336	0.0311	0.0262	0.0283	
28	0.0118	0.0110	0.0093	0.0099	
30	0.0038	0.0035	0.0030	0.0032	
32	0.0011	0.0011	0.0009	0.0010	
34	0.0003	0.0003	0.0002	0.0003	
36	0.0001	0.0001	0.0001	0.0001	
38	0.0000	0.0000	0.0000	0.0000	
40	0.0000	0.0000	0.0000	0.0000	
42	0.0000	0.0000	0.0000	0.0000	
44	0.0000	0.0000	0.0000	0.0000	
46	0.0000	0.0000	0.0000	0.0000	
48	0.0000	0.0000	0.0000	0.0000	
50	0.0000	0.0000	0.0000	0.0000	
52	0.0000	0.0000	0.0000	0.0000	
J	QR	QQ	QP	OP	SR
3	3.3713	7.3689	1.0535	0.8345	5.0843
5	3.9277	10.7928	1.8883	1.5956	4.9580
7	3.8303	11.6618	2.2426	1.9565	4.5326
9	3.2805	10.5881	2.1511	1.9109	3.7597
11	2.5096	8.4114	1.7714	1.5908	2.8246
13	1.7305	5.9554	1.2864	1.1629	1.9266
15	1.0817	3.7960	0.8356	0.7583	1.1962
17	0.6152	2.1917	0.4895	0.4452	0.6776
19	0.3193	1.1509	0.2601	0.2367	0.3508
21	0.1515	0.5513	0.1258	0.1145	0.1663
23	0.0658	0.2414	0.0555	0.0505	0.0722
25	0.0262	0.0968	0.0224	0.0203	0.0288
27	0.0096	0.0356	0.0083	0.0075	0.0105
29	0.0032	0.0120	0.0028	0.0025	0.0035
31	0.0010	0.0037	0.0009	0.0008	0.0011
33	0.0003	0.0011	0.0002	0.0002	0.0003
35	0.0001	0.0003	0.0001	0.0001	0.0001
37	0.0000	0.0001	0.0000	0.0000	0.0000
39	0.0000	0.0000	0.0000	0.0000	0.0000
41	0.0000	0.0000	0.0000	0.0000	0.0000
43	0.0000	0.0000	0.0000	0.0000	0.0000
45	0.0000	0.0000	0.0000	0.0000	0.0000
47	0.0000	0.0000	0.0000	0.0000	0.0000
49	0.0000	0.0000	0.0000	0.0000	0.0000
51	0.0000	0.0000	0.0000	0.0000	0.0000

Table VIII continued

- 17 -

0,1 BAND TEMP 200°K					
J	RR	RQ	PP	PQ	
2	4.1768	1.3935	0.4610	0.9228	
4	4.5383	2.7255	1.4347	2.1542	
6	4.5246	3.2349	2.0415	2.7246	
8	4.0272	3.1352	2.1769	2.7236	
10	3.2160	2.6338	1.9377	2.3274	
12	2.3183	1.9635	1.5006	1.7523	
14	1.5155	1.3148	1.0316	1.1800	
16	0.9015	0.7963	0.6366	0.7168	
18	0.4893	0.4382	0.3551	0.3949	
20	0.2427	0.2198	0.1799	0.1981	
22	0.1102	0.1008	0.0831	0.0907	
24	0.0459	0.0423	0.0350	0.0380	
26	0.0175	0.0163	0.0135	0.0146	
28	0.0062	0.0057	0.0048	0.0051	
30	0.0020	0.0019	0.0016	0.0017	
32	0.0006	0.0006	0.0005	0.0005	
34	0.0002	0.0002	0.0001	0.0001	
36	0.0000	0.0000	0.0000	0.0000	
38	0.0000	0.0000	0.0000	0.0000	
40	0.0000	0.0000	0.0000	0.0000	
42	0.0000	0.0000	0.0000	0.0000	
44	0.0000	0.0000	0.0000	0.0000	
46	0.0000	0.0000	0.0000	0.0000	
48	0.0000	0.0000	0.0000	0.0000	
50	0.0000	0.0000	0.0000	0.0000	
52	0.0000	0.0000	0.0000	0.0000	
J	QR	QQ	QP	OP	SR
3	1.7431	3.8093	0.5447	0.4305	2.6321
5	2.0310	5.5799	0.9764	0.8223	2.5696
7	1.9809	6.0300	1.1598	1.0075	2.3519
9	1.6969	5.4759	1.1127	0.9832	1.9531
11	1.2984	4.3512	0.9165	0.8178	1.4692
13	0.8956	3.0816	0.6658	0.5974	1.0034
15	0.5600	1.9649	0.4326	0.3893	0.6238
17	0.3186	1.1349	0.2535	0.2284	0.3538
19	0.1654	0.5962	0.1347	0.1214	0.1835
21	0.0785	0.2857	0.0652	0.0586	0.0871
23	0.0341	0.1252	0.0288	0.0258	0.0379
25	0.0136	0.0502	0.0116	0.0104	0.0151
27	0.0050	0.0185	0.0043	0.0038	0.0055
29	0.0017	0.0062	0.0015	0.0013	0.0019
31	0.0005	0.0019	0.0005	0.0004	0.0006
33	0.0001	0.0006	0.0001	0.0001	0.0002
35	0.0000	0.0001	0.0000	0.0000	0.0000
37	0.0000	0.0000	0.0000	0.0000	0.0000
39	0.0000	0.0000	0.0000	0.0000	0.0000
41	0.0000	0.0000	0.0000	0.0000	0.0000
43	0.0000	0.0000	0.0000	0.0000	0.0000
45	0.0000	0.0000	0.0000	0.0000	0.0000
47	0.0000	0.0000	0.0000	0.0000	0.0000
49	0.0000	0.0000	0.0000	0.0000	0.0000
51	0.0000	0.0000	0.0000	0.0000	0.0000

Table VIII continued

- 18 -

0,0 BAND TEMP 250°K					
J	RR	RQ	PP	PQ	
2	8.1753	2.7270	0.9034	1.8082	
4	9.1350	5.4850	2.8945	4.3451	
6	9.5193	6.8046	4.3094	5.7501	
8	9.0012	7.0063	4.8867	6.1129	
10	7.7616	6.3553	4.7016	5.6461	
12	6.1403	5.1997	4.0000	4.6700	
14	4.4774	3.8835	3.0701	3.5112	
16	3.0194	2.6663	2.1499	2.4203	
18	1.8879	1.6906	1.3832	1.5380	
20	1.0967	0.9930	0.8214	0.9042	
22	0.5927	0.5416	0.4517	0.4931	
24	0.2984	0.2747	0.2306	0.2500	
26	0.1401	0.1298	0.1095	0.1180	
28	0.0614	0.0572	0.0484	0.0519	
30	0.0251	0.0235	0.0199	0.0213	
32	0.0096	0.0090	0.0077	0.0082	
34	0.0034	0.0032	0.0028	0.0029	
36	0.0011	0.0011	0.0009	0.0010	
38	0.0004	0.0003	0.0003	0.0003	
40	0.0001	0.0001	0.0001	0.0001	
42	0.0000	0.0000	0.0000	0.0000	
44	0.0000	0.0000	0.0000	0.0000	
46	0.0000	0.0000	0.0000	0.0000	
48	0.0000	0.0000	0.0000	0.0000	
50	0.0000	0.0000	0.0000	0.0000	
52	0.0000	0.0000	0.0000	0.0000	
J	QR	QQ	QP	OP	SR
3	3.4549	7.5515	1.0796	0.8552	5.2103
5	4.1755	11.4739	2.0074	1.6963	5.2708
7	4.2938	13.0729	2.5140	2.1933	5.0811
9	3.9414	12.7213	2.5845	2.2959	4.5171
11	3.2847	11.0094	2.3186	2.0821	3.6970
13	2.5080	8.6310	1.8644	1.6854	2.7921
15	1.7643	6.1914	1.3628	1.2368	1.9511
17	1.1478	4.0889	0.9132	0.8306	1.2642
19	0.6924	2.4962	0.5640	0.5134	0.7609
21	0.3881	1.4127	0.3222	0.2933	0.4261
23	0.2024	0.7428	0.1708	0.1553	0.2222
25	0.0984	0.3634	0.0841	0.0764	0.1081
27	0.0446	0.1656	0.0385	0.0349	0.0490
29	0.0189	0.0704	0.0165	0.0149	0.0208
31	0.0075	0.0279	0.0066	0.0059	0.0082
33	0.0028	0.0104	0.0024	0.0022	0.0030
35	0.0010	0.0036	0.0008	0.0008	0.0011
37	0.0003	0.0012	0.0003	0.0002	0.0003
39	0.0001	0.0004	0.0001	0.0001	0.0001
41	0.0000	0.0001	0.0000	0.0000	0.0000
43	0.0000	0.0000	0.0000	0.0000	0.0000
45	0.0000	0.0000	0.0000	0.0000	0.0000
47	0.0000	0.0000	0.0000	0.0000	0.0000
49	0.0000	0.0000	0.0000	0.0000	0.0000
51	0.0000	0.0000	0.0000	0.0000	0.0000

Table VIII continued

- 19 -

0.1 BAND TEMP 250°K					
J	RR	RQ	PP	PQ	
2	4.2282	1.4107	0.4666	0.9342	
4	4.7273	2.8390	1.4945	2.2439	
6	4.9293	3.5242	2.2241	2.9683	
8	4.6641	3.6311	2.5212	3.1544	
10	4.0247	3.2961	2.4250	2.9127	
12	3.1864	2.6988	2.0626	2.4085	
14	2.3253	2.0173	1.5828	1.8105	
16	1.5694	1.3862	1.1082	1.2478	
18	0.9822	0.8797	0.7129	0.7928	
20	0.5711	0.5172	0.4233	0.4661	
22	0.3089	0.2824	0.2328	0.2542	
24	0.1557	0.1434	0.1188	0.1289	
26	0.0732	0.0678	0.0564	0.0608	
28	0.0321	0.0299	0.0249	0.0267	
30	0.0131	0.0123	0.0103	0.0110	
32	0.0050	0.0047	0.0040	0.0042	
34	0.0018	0.0017	0.0014	0.0015	
36	0.0006	0.0006	0.0005	0.0005	
38	0.0002	0.0002	0.0001	0.0002	
40	0.0001	0.0001	0.0000	0.0000	
42	0.0000	0.0000	0.0000	0.0000	
44	0.0000	0.0000	0.0000	0.0000	
46	0.0000	0.0000	0.0000	0.0000	
48	0.0000	0.0000	0.0000	0.0000	
50	0.0000	0.0000	0.0000	0.0000	
52	0.0000	0.0000	0.0000	0.0000	
J	QR	QQ	QP	OP	SR
3	1.7863	3.9037	0.5582	0.4412	2.6973
5	2.1591	5.9320	1.0380	0.8742	2.7317
7	2.2206	6.7596	1.3002	1.1294	2.6364
9	2.0387	6.5791	1.3369	1.1812	2.3466
11	1.6995	5.6951	1.1996	1.0704	1.9229
13	1.2980	4.4660	0.9649	0.8658	1.4541
15	0.9134	3.2047	0.7056	0.6349	1.0174
17	0.5944	2.1172	0.4730	0.4261	0.6601
19	0.3588	1.2931	0.2922	0.2632	0.3979
21	0.2012	0.7322	0.1670	0.1503	0.2231
23	0.1050	0.3851	0.0886	0.0795	0.1165
25	0.0510	0.1885	0.0436	0.0391	0.0568
27	0.0231	0.0860	0.0200	0.0179	0.0258
29	0.0098	0.0366	0.0086	0.0076	0.0109
31	0.0039	0.0145	0.0034	0.0030	0.0043
33	0.0014	0.0054	0.0013	0.0011	0.0016
35	0.0005	0.0019	0.0004	0.0004	0.0006
37	0.0002	0.0006	0.0001	0.0001	0.0002
39	0.0000	0.0002	0.0000	0.0000	0.0001
41	0.0000	0.0001	0.0000	0.0000	0.0000
43	0.0000	0.0000	0.0000	0.0000	0.0000
45	0.0000	0.0000	0.0000	0.0000	0.0000
47	0.0000	0.0000	0.0000	0.0000	0.0000
49	0.0000	0.0000	0.0000	0.0000	0.0000
51	0.0000	0.0000	0.0000	0.0000	0.0000

Table VIII continued

- 20 -

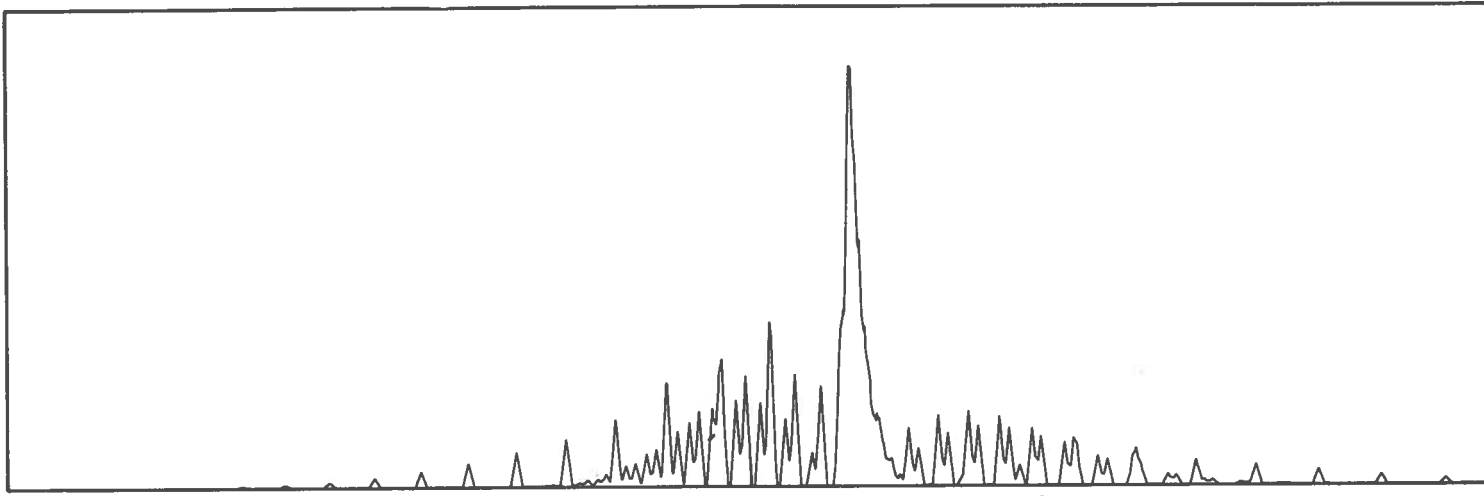
## 0,0 BAND TEMP 300°K

J	RR	RQ	PP	PQ	
2	8.2423	2.7494	0.9108	1.8231	
4	9.3868	5.6363	2.9743	4.4649	
6	10.0788	7.2046	4.5626	6.0881	
8	9.9269	7.7269	5.3893	6.7416	
10	9.0136	7.3805	5.4600	6.5569	
12	7.5907	6.4279	4.9448	5.7731	
14	5.9562	5.1661	4.0841	4.6709	
16	4.3694	3.8585	3.1111	3.5025	
18	3.0044	2.6903	2.2011	2.4474	
20	1.9399	1.7566	1.4531	1.5595	
22	1.1781	1.0765	0.8979	0.9802	
24	0.6737	0.6203	0.5206	0.5644	
26	0.3631	0.3365	0.2837	0.3057	
28	0.1846	0.1720	0.1455	0.1560	
30	0.0886	0.0829	0.0703	0.0751	
32	0.0402	0.0378	0.0321	0.0341	
34	0.0172	0.0162	0.0138	0.0146	
36	0.0070	0.0066	0.0056	0.0059	
38	0.0027	0.0025	0.0022	0.0023	
40	0.0010	0.0009	0.0008	0.0008	
42	0.0003	0.0003	0.0003	0.0003	
44	0.0001	0.0001	0.0001	0.0001	
46	0.0000	0.0000	0.0000	0.0000	
48	0.0000	0.0000	0.0000	0.0000	
50	0.0000	0.0000	0.0000	0.0000	
52	0.0000	0.0000	0.0000	0.0000	
J	QR	QQ	QP	OP	SR
3	3.5117	6.6758	1.0974	0.8693	5.2960
5	4.3494	11.9516	2.0910	1.7669	5.4903
7	4.6335	14.1072	2.7129	2.3668	5.4831
9	4.4544	14.3771	2.9209	2.5947	5.1051
11	3.9303	13.1733	2.7743	2.4914	4.4236
13	3.2119	11.0533	2.3876	2.1584	3.5757
15	2.4447	8.5788	1.8883	1.7138	2.7034
17	1.7395	6.1966	1.3840	1.2587	1.9158
19	1.1602	4.1825	0.9450	0.8602	1.2750
21	0.7268	2.6455	0.6034	0.5492	0.7979
23	0.4282	1.5714	0.3612	0.3285	0.4701
25	0.2376	0.8779	0.2032	0.1845	0.2611
27	0.1243	0.4619	0.1075	0.0975	0.1367
29	0.0613	0.2291	0.0536	0.0485	0.0676
31	0.0286	0.1072	0.0252	0.0227	0.0316
33	0.0126	0.0474	0.0112	0.0101	0.0139
35	0.0052	0.0198	0.0047	0.0042	0.0058
37	0.0021	0.0078	0.0019	0.0017	0.0023
39	0.0008	0.0029	0.0007	0.0006	0.0009
41	0.0003	0.0010	0.0002	0.0002	0.0003
43	0.0001	0.0003	0.0001	0.0001	0.0001
45	0.0000	0.0001	0.0000	0.0000	0.0000
47	0.0000	0.0000	0.0000	0.0000	0.0000
49	0.0000	0.0000	0.0000	0.0000	0.0000
51	0.0000	0.0000	0.0000	0.0000	0.0000

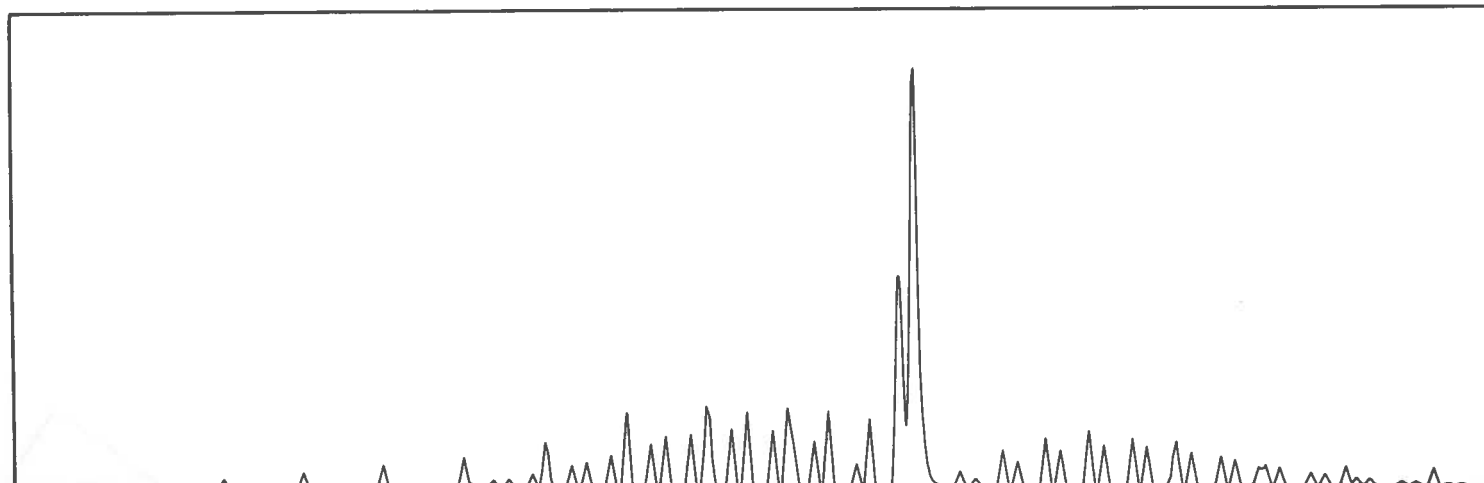
Table VIII continued

- 21 -

J	0,1 BAND TEMP 300°K				
	RR	RQ	PP	PQ	
2	4.2628	1.4222	0.4705	0.9419	
4	4.8576	2.9173	1.5357	2.3057	
6	5.2190	3.7314	2.3548	3.1427	
8	5.1438	4.0046	2.7805	3.4789	
10	4.6739	3.8278	2.8162	3.3825	
12	3.9391	3.3363	2.5498	2.9775	
14	3.0934	2.6836	2.1055	2.4085	
16	2.2712	2.0060	1.6037	1.8057	
18	1.5630	1.3999	1.1345	1.2616	
20	1.0102	0.9149	0.7489	0.8245	
22	0.6141	0.5612	0.4627	0.5052	
24	0.3515	0.3237	0.2683	0.2909	
26	0.1896	0.1758	0.1462	0.1576	
28	0.0965	0.0900	0.0750	0.0804	
30	0.0464	0.0434	0.0363	0.0387	
32	0.0210	0.0198	0.0165	0.0176	
34	0.0090	0.0085	0.0071	0.0075	
36	0.0037	0.0035	0.0029	0.0031	
38	0.0014	0.0013	0.0011	0.0012	
40	0.0005	0.0005	0.0004	0.0004	
42	0.0002	0.0002	0.0001	0.0001	
44	0.0001	0.0001	0.0000	0.0000	
46	0.0000	0.0000	0.0000	0.0000	
48	0.0000	0.0000	0.0000	0.0000	
50	0.0000	0.0000	0.0000	0.0000	
52	0.0000	0.0000	0.0000	0.0000	
J	QR	QQ	QP	OP	SR
3	1.8157	3.9679	0.5674	0.4484	2.7417
5	2.2490	6.1789	1.0813	0.9106	2.8455
7	2.3963	7.2945	1.4030	1.2187	2.8450
9	2.3041	7.4354	1.5109	1.3350	2.6521
11	2.0335	6.8144	1.4354	1.2808	2.3009
13	1.6622	5.7194	1.2357	1.1087	1.8622
15	1.2656	4.4404	0.9776	0.8797	1.4098
17	0.9009	3.2086	0.7168	0.6457	1.0004
19	0.6011	2.1666	0.4896	0.4410	0.6667
21	0.3767	1.3710	0.3128	0.2814	0.4178
23	0.2221	0.8148	0.1873	0.1682	0.2465
25	0.1233	0.4554	0.1054	0.0944	0.1371
27	0.0645	0.2398	0.0558	0.0499	0.0719
29	0.0319	0.1190	0.0278	0.0248	0.0356
31	0.0149	0.0557	0.0131	0.0116	0.0167
33	0.0065	0.0246	0.0058	0.0051	0.0074
35	0.0027	0.0103	0.0024	0.0021	0.0031
37	0.0011	0.0041	0.0010	0.0008	0.0012
39	0.0004	0.0015	0.0004	0.0003	0.0005
41	0.0001	0.0005	0.0001	0.0001	0.0002
43	0.0000	0.0002	0.0000	0.0000	0.0001
45	0.0000	0.0001	0.0000	0.0000	0.0000
47	0.0000	0.0000	0.0000	0.0000	0.0000
49	0.0000	0.0000	0.0000	0.0000	0.0000
51	0.0000	0.0000	0.0000	0.0000	0.0000

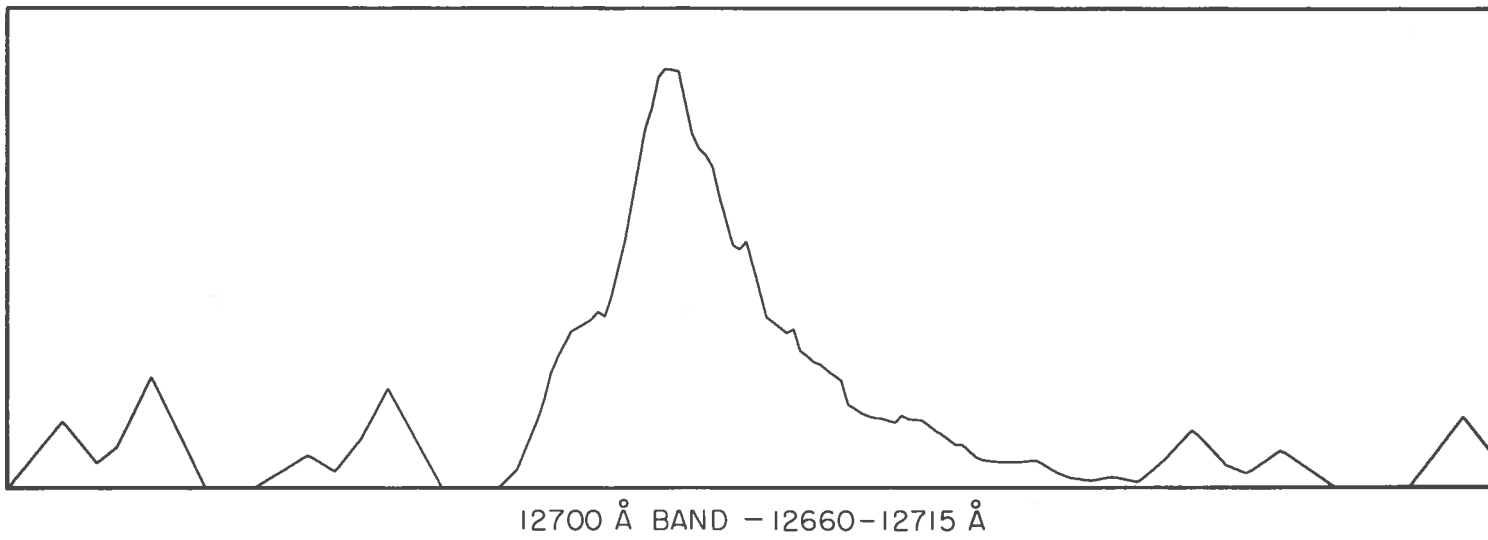


12700 Å BAND - 12400-12900 Å

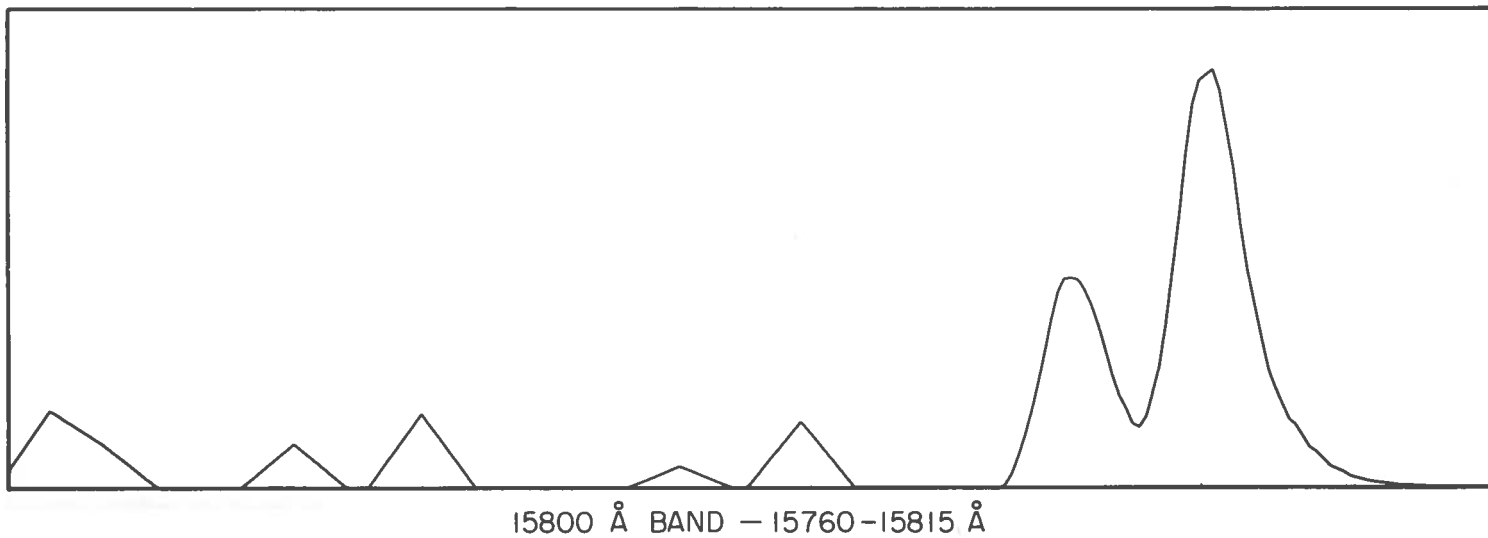


15800 Å BAND - 15500-16000 Å

*Fig. 2 Theoretical spectrum of the 0,0 and 0,1 bands at 250°K after convolution with a triangular function with a full width of 2 Å at half-height.*



12700 Å BAND - 12660-12715 Å



15800 Å BAND - 15760-15815 Å

*Fig. 3 Theoretical spectrum of the central portion of the 0,0 and 0,1 bands at 250°K after convolution with a triangular function with a full width of 2 Å at half-height.*

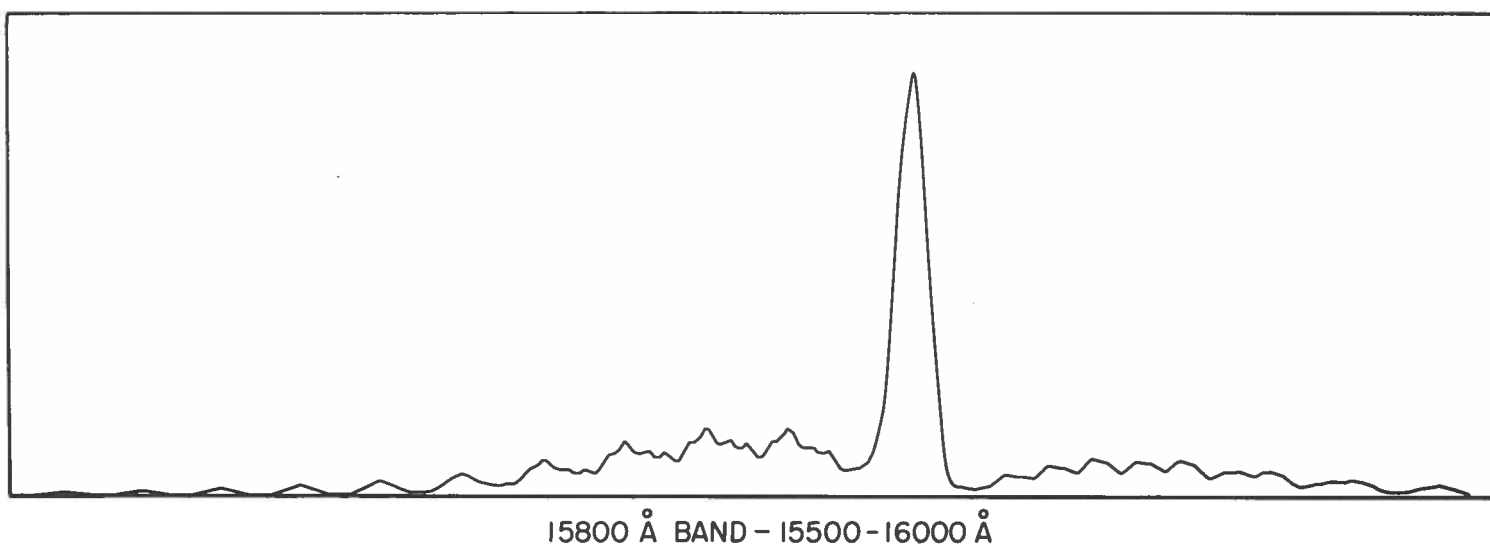
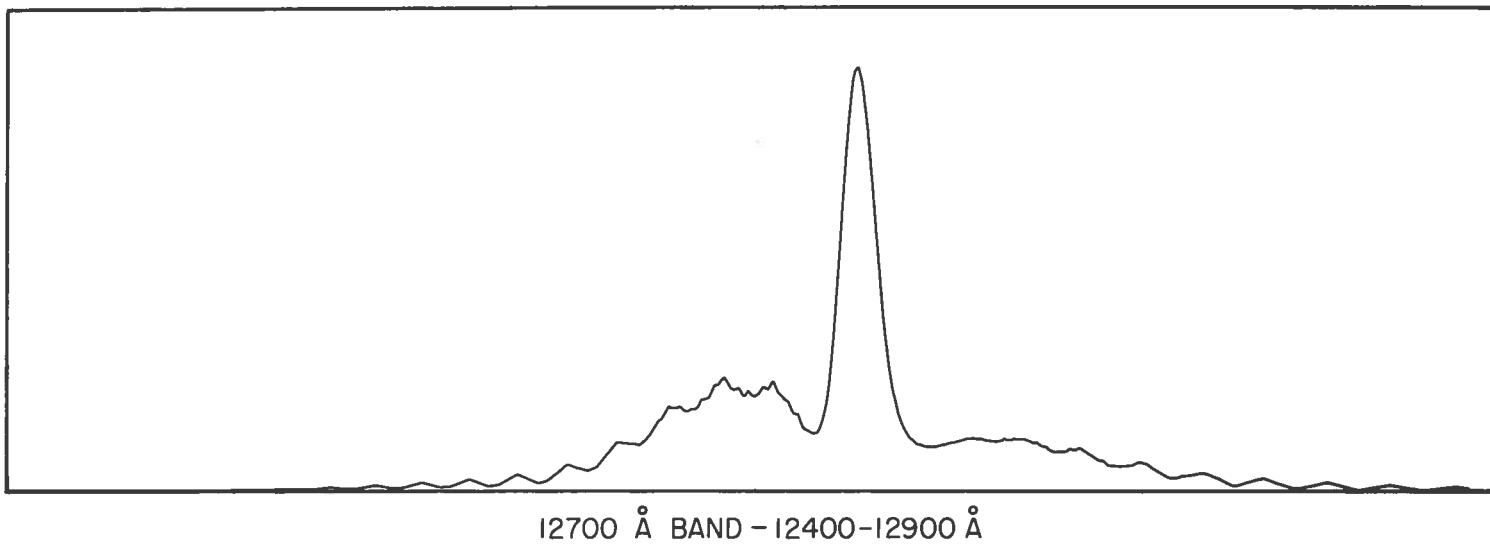
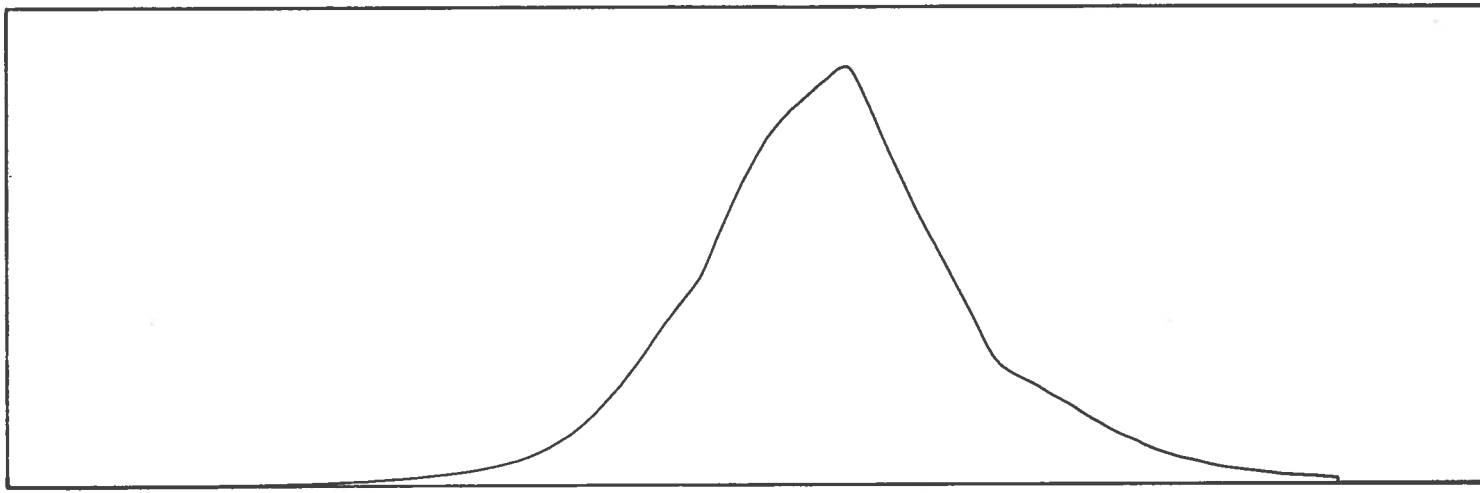
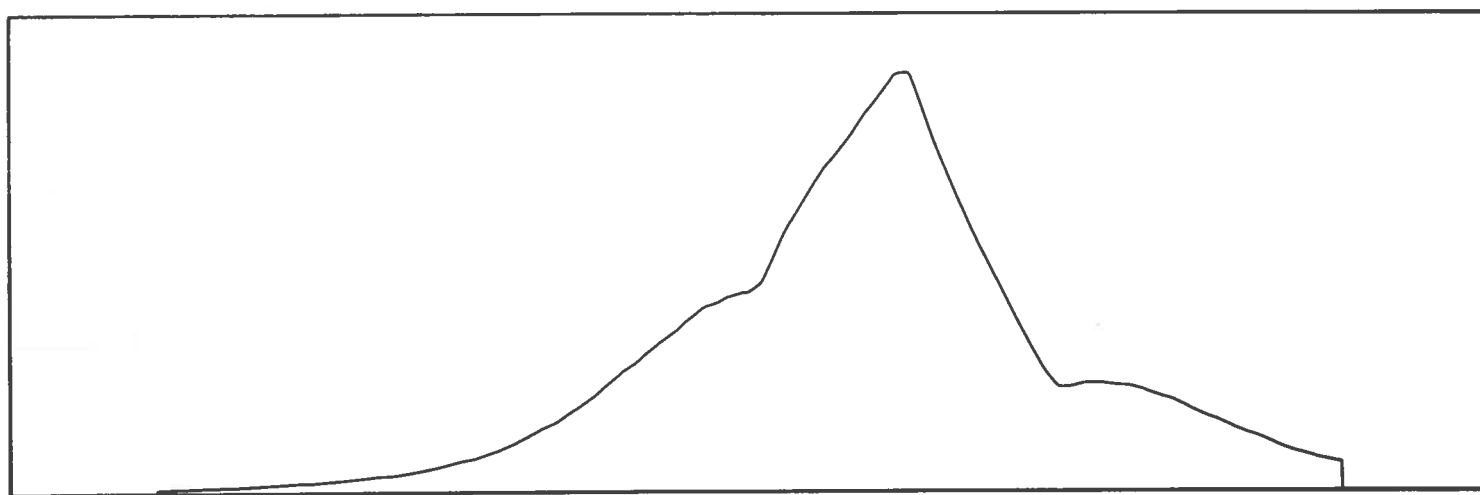


Fig. 4 Theoretical spectrum of the 0,0 and 0,1 bands at 300°K after convolution with a triangular function with a full width of 10 $\text{\AA}$  at half-height.



12700  $\text{\AA}$  BAND — 12400–12900  $\text{\AA}$



15800  $\text{\AA}$  BAND — 15500–16000  $\text{\AA}$

Fig. 5 Theoretical spectrum of the 0,0 and 0,1 bands at 200°K after convolution with a triangular function with a full width of 50 $\text{\AA}$  at half-height.

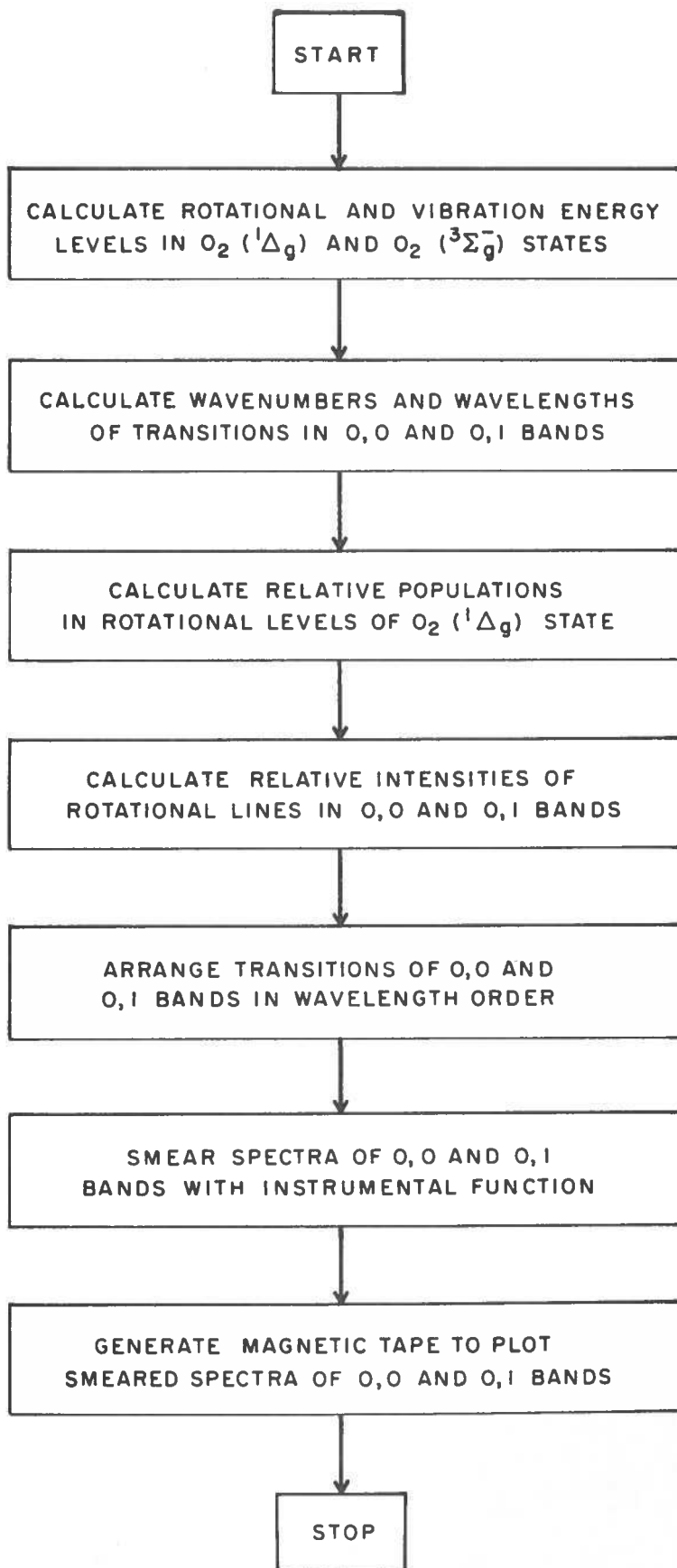


Fig. 6 Flow chart of the computer program written to solve the equations describing the band structure in the  $O_2(^1\Delta_g - ^3\Sigma_g^-)$  system